

Large Tunneling Anisotropic Magnetoresistance in (Ga,Mn)As Nanoconstrictions

A. D. Giddings,^{1,2} M. N. Khalid,² T. Jungwirth,^{3,1} J. Wunderlich,² S. Yasin,⁴ R. P. Campion,¹ K. W. Edmonds,¹ J. Sinova,⁵
K. Ito,² K.-Y. Wang,¹ D. Williams,² B. L. Gallagher,¹ and C. T. Foxon¹

¹*School of Physics and Astronomy, University of Nottingham, Nottingham NG7 2RD, United Kingdom*

²*Hitachi Cambridge Laboratory, Cambridge CB3 0HE, United Kingdom*

³*Institute of Physics ASCR, Cukrovarnická 10, 162 53 Praha 6, Czech Republic*

⁴*Microelectronics Research Centre, Cavendish Laboratory, University of Cambridge, Cambridge CB3 0HE, United Kingdom*

⁵*Department of Physics, Texas A&M University, College Station, Texas 77843-4242, USA*

(Received 8 September 2004; revised manuscript received 7 December 2004; published 30 March 2005)

We report a large tunneling anisotropic magnetoresistance (TAMR) in (Ga,Mn)As lateral nanoconstrictions. Unlike previously reported tunneling magnetoresistance effects in nanocontacts, the TAMR does not require noncollinear magnetization on either side of the constriction. The nature of the effect is established by a direct comparison of its phenomenology with that of normal anisotropic magnetoresistance (AMR) measured in the same lateral geometry. The direct link we establish between the TAMR and AMR indicates that TAMR may be observable in other materials showing room temperature AMR and demonstrates that the physics of nanoconstriction magnetoresistive devices can be much richer than previously thought.

DOI: 10.1103/PhysRevLett.94.127202

PACS numbers: 75.50.Pp, 85.75.Mm

The family of (III,Mn)V ferromagnetic semiconductors offers unique opportunities for exploring the integration of two frontier areas in information technology: spintronics and nanoelectronics. Striking examples of the synergy of the two fields are the giant magnetoresistance and the tunnel magnetoresistance (TMR) effects recently observed [1] in lithographically defined (Ga, Mn)As nanoconstrictions. The former effect, measured in larger size diffusive constrictions and reminiscent of previous magnetotransport studies in metallic nanocontacts [2,3], is interpreted in terms of scattering off domain walls pinned at the nanoconstrictions. The smaller sub-10 nm contacts, acting as tunnel barriers, led to a full magnetic decoupling of the leads and the resulting $\sim 2000\%$ effect arises from variation of the relative orientation of the magnetization on either side of the constriction [1]. This discovery is clearly of great importance as the size of the effect indicates that nanospintronic structures may provide a new route to memory and sensor devices.

In this Letter we report large magnetoresistance (MR) in (Ga, Mn)As lateral nanoconstrictions whose geometry and crystal orientation diminish the role of either the domain-wall resistance or the TMR effect. We demonstrate a direct link between the normal anisotropic magnetoresistance (AMR) [4,5] of unstructured bars and the MR effects observed in our tunneling nanoconstrictions, establishing their tunneling anisotropic magnetoresistance (TAMR) origin. This novel phenomenon arises from the spin-orbit (SO) coupling, much like the AMR, and reflects the dependence of the tunneling density of states of the ferromagnetic layer on the orientation of the magnetization with respect to the current direction or the crystallographic axes. The TAMR effect was discovered [6] only recently in a (Ga, Mn)As/AlOx/Au vertical tunneling device. By using a fully epitaxial (Ga, Mn)As/GaAs/(Ga, Mn)As stack it

has very recently been demonstrated that TAMR can exceed 100 000% [7] at temperature 1.7 K. Our observation of TAMR in lateral constrictions enriches the field of nanocontact spin phenomena by a new MR effect. The demonstration of the direct link to AMR, which is a MR effect present also in many metallic ferromagnets [8], may have important implications beyond the area of currently low Curie temperature ferromagnetic semiconductors.

The geometry of the devices is shown in Fig. 1(a). All devices discussed in this Letter were fabricated from a single Ga_{0.98}Mn_{0.02}As epilayer grown along the [001] crystal axis by low-temperature molecular beam epitaxy [9]. Despite being only 5 nm thick, the layer has a Curie temperature of 40 K and room temperature conductivity $130 \Omega^{-1} \text{cm}^{-1}$: values comparable with those achieved in thicker layers for 2% Mn. Device fabrication was carried out by e-beam lithography using poly(methyl methacrylate) positive resist and reactive ion etching. The 3 μm wide Hall bar, aligned along the [110] direction, has pairs of constrictions from 30 to 400 nm wide separated by a distance of 9 μm . For reference AMR experiments, a separate bar without constrictions was fabricated in parallel to the stripe. Four point *I-V* curves and resistances were measured for both the unstructured Hall bars and the constrictions. Low frequency lock-in techniques were used to maximize the signal to noise ratio.

Figure 1(b) shows MR characteristics for external magnetic field applied parallel to the current direction. The unstructured bar and the 100 nm constrictions show MRs typical of (Ga, Mn)As epilayers [4]. The isotropic (independent of applied field orientation) negative part of the MR in these traces is attributed to the suppression of magnetic disorder at large fields [4]. The hysteretic low-field effect is associated with magnetization reversal and since its magnitude and sense change with applied field

orientation it is a manifestation of the AMR. The MR for the 50 nm constriction partly deviates from this normal bulk (Ga, Mn)As behavior and a dramatic change is observed for the 30 nm constriction, both in the size and the sign of the low-field effect. The measured temperature dependent I - V curves of Fig. 1(c) show that the appearance of these anomalies is related to the formation of a tunnel junction. Constrictions greater than 100 nm show Ohmic behavior. Deviations from Ohmic behavior become more pronounced as constriction size and temperature are reduced. At low temperature and bias, conduction through the 30 nm constrictions is by tunneling. The occurrence of tunneling in such a wide constriction suggests that disorder in the very thin, low Mn density, (Ga, Mn)As material leads to local depletion and a tunnel barrier of lateral width considerably smaller than the nominal physical width.

The negative sign of the hysteretic effect in our tunneling device is not compatible with TMR, for which anti-parallel alignment on either side of the constriction at intermediate fields would lead to a positive hysteretic effect in the present geometry. Instead, we interpret the data as TAMR, which can give both normal and inverted spin-valve-like behavior depending on the applied field orientation [6,7].

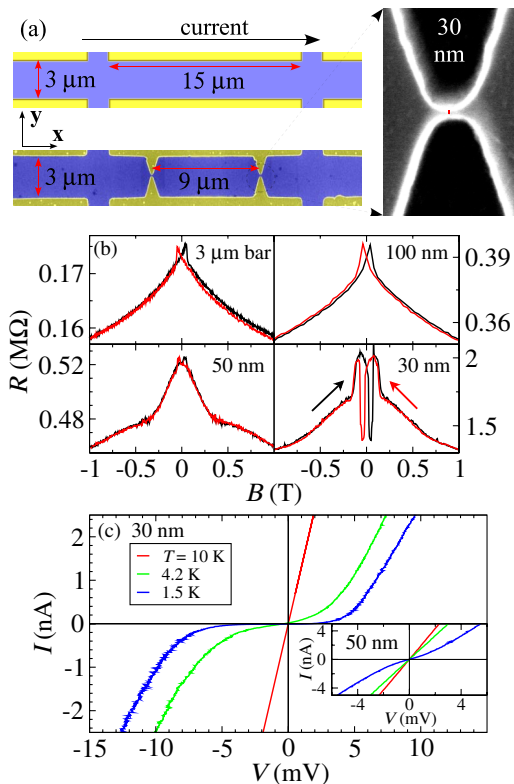


FIG. 1 (color online). (a) Schematic of the unstructured bar and scanning electron microscopy image of a double constricted nanodevice. (b) MR measurements for unconstricted (upper left panel) and constricted devices for $\mathbf{B} \parallel \mathbf{x}$ at a temperature of 4.2 K (c) I - V characteristics for the 30 and 50 nm constrictions.

In Fig. 2 we plot the AMR characteristics of the unstructured bar for magnetic fields applied parallel to the stripe ($\mathbf{B} \parallel \mathbf{x}$), perpendicular to the stripe in plane ($\mathbf{B} \parallel \mathbf{y}$), and perpendicular to the stripe out-of-plane ($\mathbf{B} \parallel \mathbf{z}$). From SQUID magnetometry measurements we find in our (Ga, Mn)As epilayers the previously reported competition between [100]([010]) biaxial and [110] uniaxial easy axes [10]. At 4.2 K biaxial anisotropy dominates and for the [110] oriented bars magnetization reversal can proceed via stable intermediate [100] or [010] orientations [11]. We interpret the positive (negative) going hysteretic features in Fig. 2 for $\mathbf{B} \parallel \mathbf{x}$ ($\mathbf{B} \parallel \mathbf{y}$) as rotation of the magnetization from [110] ($\bar{1}\bar{1}0$) into an orientation close to a [100] (or [010]) easy axis, consistent with $\mathbf{M} \parallel \mathbf{x}$ being a low resistance state and $\mathbf{M} \parallel \mathbf{y}$ being a high resistance state [4,5].

A much stronger MR is observed for $\mathbf{B} \parallel \mathbf{z}$ than for $\mathbf{B} \parallel \mathbf{y}$. Assuming that the magnetization is saturated along the direction of the applied field at 1 T we obtain from the data of the inset of Fig. 2 $(R(\mathbf{M} \parallel \mathbf{z}) - R(\mathbf{M} \parallel \mathbf{x}))/R(\mathbf{M} \parallel \mathbf{x}) = 12\%$ while $(R(\mathbf{M} \parallel \mathbf{y}) - R(\mathbf{M} \parallel \mathbf{x}))/R(\mathbf{M} \parallel \mathbf{x}) = 5\%$. In previously studied $\text{Ga}_{0.98}\text{Mn}_{0.02}\text{As}$ epilayers there was virtually no difference in the MRs for the two perpendicular-to-current orientations [5]. The large out-of-plane MR we observe is therefore attributed to the strong vertical confinement of the carriers in our ultrathin $\text{Ga}_{0.98}\text{Mn}_{0.02}\text{As}$ epilayer which breaks the symmetry between states with magnetization $\mathbf{M} \parallel \mathbf{y}$ and $\mathbf{M} \parallel \mathbf{z}$. Another indication of confinement effects is the presence of hysteresis in the $\mathbf{B} \parallel \mathbf{z}$ MR. In thicker (Ga, Mn)As epilayers the growth direction is magnetically hard with zero remanence due to compressive strain induced by the GaAs substrate and shape anisotropy [12]. These effects compete in our epilayer with

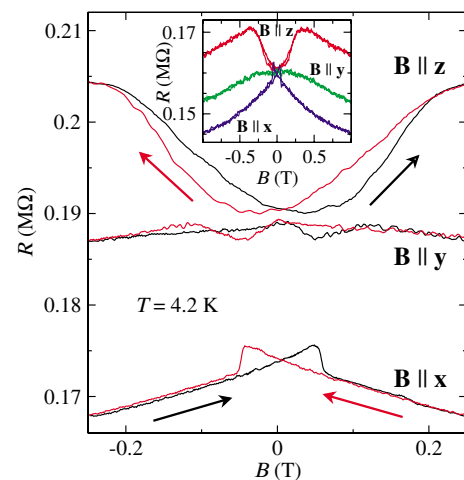


FIG. 2 (color online). Low-field ac MR measurements for the unstructured bar with applied field in three orthogonal orientations at a temperature of 4.2 K. The inset shows dc MR measurements for a wider field range. As discussed in the text, the ac measurements have a good signal to noise ratio but are affected by spurious resistance offsets. The offsets are absent in the dc measurements but the signal to noise ratio is poorer obscuring low-field hysteretic behavior.

an increase in the relative population of the heavy hole states due to the confinement, which tends to favor spin polarization along the growth direction [13].

Note that the low-field ac measurements in the main panel of Fig. 2 have a good signal to noise ratio but are affected by spurious resistance offsets leading to apparent splittings of the MRs at low fields, especially so for the $\mathbf{B} \parallel \mathbf{x}$ orientation. The offsets are absent in the dc measurements, shown in the inset, but the signal to noise is significantly poorer obscuring the hysteretic behavior. The field-independent offsets occur entirely as a consequence of the ac-field lock-in technique and of the thermal cycling of the sample (*in situ* rotation from $\mathbf{B} \parallel \mathbf{y}$ to $\mathbf{B} \parallel \mathbf{x}$ is not possible in our setup) and the shape of the individual MR curves is fully reproducible.

The dominance of the TAMR effect in the tunneling regime in our devices is clearly demonstrated in Fig. 3. This shows that the measured MR is different for the three orthogonal applied field directions. The field-independent offsets in the ac measurements, having the same origin as in the ac AMR experiment, do not allow us to determine accurately the size of the TAMR; however, an order of magnitude increase of the anisotropic MR in the tunneling regime is clearly visible from the $\mathbf{M} \parallel \mathbf{z}$ and $\mathbf{M} \parallel \mathbf{y}$ traces in the left inset of Figs. 3. The right inset of Fig. 3 shows

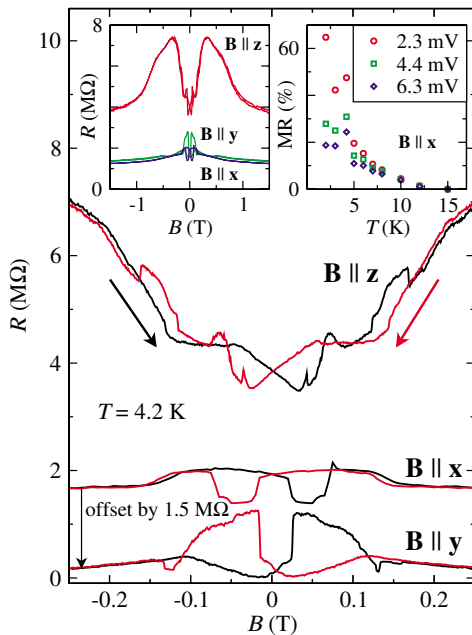


FIG. 3 (color online). Low-field ac MR measurement of the 30 nm constriction with applied field in the three orthogonal directions. The $\mathbf{B} \parallel \mathbf{y}$ curve is offset downwards by 1.5 M Ω for clarity. All MR traces shown were measured at a current of 1 nA. This may have led to a relative suppression of the magnitude of the measured MR response for $\mathbf{B} \parallel \mathbf{z}$ relative to $\mathbf{B} \parallel \mathbf{x}$ and $\mathbf{B} \parallel \mathbf{y}$ MR responses due to the non-Ohmic I - V characteristics of the tunnel constrictions. Left inset: Measured ac MRs for a wider field range. Right inset: the temperature dependence of the hysteretic low-field MR for three different voltages, with $\mathbf{B} \parallel \mathbf{x}$.

that the magnitude of the hysteretic low-field MR for $\mathbf{B} \parallel \mathbf{x}$ increases strongly as temperature and excitation voltage are reduced, consistent with the increasing dominance of tunneling.

The close correspondence between the AMR results of Fig. 2 and the TAMR results of Fig. 3 is evident. The switching events in the in-plane MR traces occur at comparable magnetic fields for the two devices. In both experiments, the hysteretic effects for $\mathbf{B} \parallel \mathbf{x}$ and $\mathbf{B} \parallel \mathbf{y}$ have similar magnitudes but opposite sign. (Note that the high and low resistance states switch places in the AMR and TAMR traces which is not surprising given the different transport regimes of the two devices.) A particularly important comparison is between the $\mathbf{B} \parallel \mathbf{z}$ MR traces as we expect the magnetization to be unaffected by the constriction as it approaches saturation. Indeed, the corresponding curves in Figs. 2 and 3 show the expected similarity in general form and field scale. The observation that in both the unstructured bar and in the tunneling constrictions the MR is considerably larger for $\mathbf{B} \parallel \mathbf{z}$ than for in-plane fields is another manifestation of the link between the AMR and TAMR effects. Hysteretic MR responses in the unstructured bar for purely in-plane magnetization are relatively simple to explain and can give useful information on magnetization reversal processes [11]. MR traces in the nanocontact devices can have a more complex dependence on the orientation of the magnetization with respect to the crystallographic axes and current direction [7], and our thin layers clearly have complex magnetic anisotropies. A detailed interpretation of the low-field hysteretic MR response of our nanocontacts is therefore not possible without detailed information on the magnetization reversal sequence near the constriction.

The behavior of our nanoconstrictions, dominated by the TAMR, is distinct from the TMR signal of the (Ga, Mn)As nanocontact structure reported in Ref. [1]. In the experiment of Ref. [1], the bar was oriented along the [100] easy axis and the TMR corresponded to subsequent 180° reversals in the leads and the central island. The nonsimultaneous switching on either side of the constriction resulted from the special geometry of the device in Ref. [1] in which the narrow central (Ga, Mn)As region had a significantly larger coercive field than the wider (Ga, Mn)As regions on the opposite sides of the point contacts. Also the (Ga, Mn)As layer was thicker (19 nm) excluding the additional complexities in the anisotropy energy landscape introduced by confinement effects.

The AMR in (Ga, Mn)As was successfully modeled [5] within the Boltzmann transport theory that accounts for the SO induced anisotropies with respect to the magnetization orientation in the hole group velocities and scattering rates. The TAMR has been analyzed in terms of tunneling density of state anisotropies [6,7] or by calculating the transmission coefficient anisotropies using the Landauer formalism [14,15]. Both approaches confirmed the presence of the TAMR effects. The (Ga, Mn)As band structure in these calculations is obtained using the $\mathbf{k} \cdot \mathbf{p}$ envelope

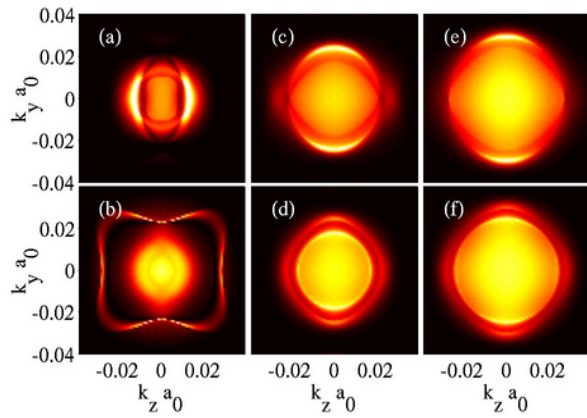


FIG. 4 (color online). Color plot of the calculated tunneling transmission probabilities vs conserved in-plane momenta at the Fermi energy. The carrier densities are 0.01 nm^{-3} (a),(b), 0.05 nm^{-3} (c),(d), and 0.1 nm^{-3} (e),(f). The barrier height is 1 eV and the width is 2 nm. White (bright yellow) is the highest probability for a given density, red (grey) the medium, and black is zero. The tunneling current is along the x direction and the magnetization is along the z direction for the first row and along the x direction for the second row.

function description of the host semiconductor valence bands in the presence of an effective kinetic-exchange field produced by the polarized local Mn moments [12].

In Fig. 4 we plot Landauer transmission probabilities at the Fermi energy as a function of conserved momenta in the (k_z, k_y) plane to illustrate the effects of confinement on the TAMR. Two semi-infinite 3D (Ga, Mn)As regions separated by a tunnel barrier are considered with the tunnel current along the x direction. In both ferromagnetic semiconductor contacts we consider substitutional Mn doping of 2% and a growth direction strain of 0.2%. Details of such calculations can be found in Ref. [15]. The additional component of the strain, which was not considered in previous Landauer transport studies, allows us to model the broken cubic symmetry effects observed in experimental TAMR [6,7]. The bulk 3D hole densities in our (Ga, Mn)As epilayer are of order $1 \times 10^{20} \text{ cm}^{-3}$ and a gradual depletion of the carriers is expected near the tunnel constriction. Data in Figs. 4(a) and 4(b) correspond to hole density $0.1 \times 10^{20} \text{ cm}^{-3}$, in Figs. 4(c) and 4(d) to density $0.5 \times 10^{20} \text{ cm}^{-3}$, and in Figs. 4(e) and 4(f) to $1 \times 10^{20} \text{ cm}^{-3}$.

The diagrams in Fig. 4 show an intricate dependence of the theoretical TAMR on the position in the (k_z, k_y) plane. When integrated over all states at the Fermi energy, the TAMR ranges between $\sim 50\%$ and $\sim 1\%$ for the studied hole densities $0.1\text{--}1 \times 10^{20} \text{ cm}^{-3}$. In the experimental structure, however, the (Ga, Mn)As is strongly confined in the growth direction which leads to depopulation of high k_z momenta states. The tunnel constriction further reduces the number of k_y states contributing to the signal. Classically, the current is carried only by particles with

small momenta in the z and y directions and wave mechanics adds a condition for minimum wave vector $k_y = \pm \pi/w$, where w is the effective width of the constriction. Figure 4 illustrates that the theoretical TAMR can change significantly depending on the k_z and k_y values selected by the confinements, which suggests that both the magnitude and sign of the effect are strongly sensitive to the detailed parameters of the tunnel barrier and of the ferromagnetic semiconductor epilayer.

To conclude, we have demonstrated the existence of the novel TAMR effect in (Ga, Mn)As nanoconstrictions and established the TAMR as a generic effect in tunnel devices with ferromagnetic contacts in which there is strong SO coupling. Our measurements open a new avenue for integration of spintronics through the TAMR effect with nano-electronics. The nanocontact TAMR effect, unlike the nanocontact TMR effect, does not require different coercive fields on either side of the nanoconstriction. The demonstration of the link between TAMR and AMR indicates that TAMR may be observable in other materials showing room temperature AMR.

The authors thank L. Eaves, A.H. MacDonald, P. Novák, M. Sawicki, L. Molenkamp, and C. Gould for useful discussions and acknowledge support from the Grant Agency and Academy of Sciences of the Czech Republic through Grant No. 202/05/0575 and Institutional Support No. AV0Z10100521, the EU FENIKS Project No. EC:G5RD-CT-2001-00535, and the UK EPSRC through Grant No. GR/S81407/01.

-
- [1] C. Rüster *et al.*, Phys. Rev. Lett. **91**, 216602 (2003).
 - [2] N. García, M. Muñoz, and Y.-W. Zhao, Phys. Rev. Lett. **82**, 2923 (1999).
 - [3] S.Z. Hua and H.D. Chopra, Phys. Rev. B **67**, 060401 (2003).
 - [4] D.V. Baxter *et al.*, Phys. Rev. B **65**, 212407 (2002).
 - [5] T. Jungwirth *et al.*, Appl. Phys. Lett. **83**, 320 (2003).
 - [6] C. Gould *et al.*, Phys. Rev. Lett. **93**, 117203 (2004).
 - [7] C. Rüster *et al.*, Phys. Rev. Lett. **94**, 027203 (2005).
 - [8] O. Jaoul, I.A. Campbell, and A. Fert, J. Magn. Magn. Mater. **5**, 23 (1977).
 - [9] R. Campion *et al.*, J. Cryst. Growth **247**, 42 (2003).
 - [10] M. Sawicki *et al.*, cond-mat/0410544 [Phys. Rev. B (to be published)].
 - [11] H.X. Tang, R.K. Kawakami, D.D. Awschalom, and M.L. Roukes, Phys. Rev. Lett. **90**, 107201 (2003).
 - [12] J. König, J. Schliemann, T. Jungwirth, and A. MacDonald, in *Electronic Structure and Magnetism of Complex Materials*, edited by D. Singh and D. Papaconstantopoulos (Springer-Verlag, Berlin, 2003).
 - [13] B. Lee, T. Jungwirth, and A. MacDonald, Semicond. Sci. Technol. **17**, 393 (2002).
 - [14] L. Brey, C. Tejedor, and J. Fernández-Rossier, Appl. Phys. Lett. **85**, 1996 (2004).
 - [15] A.G. Petukhov, A.N. Chantis, and D.O. Demchenko, Phys. Rev. Lett. **89**, 107205 (2002).